Saravana Periaswamy Sivagnanam, Adane Tilahun Getachew, Jae Hyung Choi, Yong Beom Park, Hee Chul Woo and Byung Soo Chun*

Green synthesis of silver nanoparticles from deoiled brown algal extract via Box-Behnken based design and their antimicrobial and sensing properties

DOI 10.1515/gps-2016-0052
Received March 21, 2016; accepted June 23, 2016; previously published online September 21, 2016

Abstract: The aim of this work was to acquire even and sphere-shaped silver nanoparticles (AgNPs) using statistical design of experiment. AgNPs were produced by green synthesis method using deoiled *Saccharina japonica* powder obtained after supercritical carbon dioxide ($Sc\text{-}CO_2$) extraction. Based on the Box-Behnken design, three variables influencing the size of AgNPs produced were identified as silver nitrate ($AgNO_3$) concentration, temperature, and reaction time. Optimum conditions were determined using response surface methodology for synthesis of AgNPs. We found that increasing reaction time at low concentration of $AgNO_3$ resulted in smaller particle size, and conversely increasing reaction time at high concentration of $AgNO_3$ resulted in bigger particles. The obtained AgNPs were characterized by transmission electron microscopy, energy dispersive X-ray, X-ray diffraction analysis, and ultraviolet-visible and Fourier transform infrared spectroscopy techniques for particle size, distribution, aggregation, and anisotropy. The optimum operating conditions are 1 mM of $AgNO_3$, 40°C, and 45 min with the smallest AgNPs size being 14.77 nm. The optimized AgNPs showed good antimicrobial activity and excellent sensing behavior towards hydrogen peroxide. The polyphenols present in aqueous AgNPs were evaluated by high-pressure liquid chromatography, which revealed the existence of chlorogenic acid and rutin.

***Corresponding author: Byung Soo Chun,** Department of Food Science and Technology, Pukyong National University, 45 Yongso-ro, Namgu, Busan 608-737, Korea, e-mail: bschun@pknu.ac.kr
Saravana Periaswamy Sivagnanam and Adane Tilahun Getachew: Department of Food Science and Technology, Pukyong National University, 45 Yongso-ro, Namgu, Busan 608-737, Korea. http://orcid.org/0000-0003-1260-0575 (A. Tilahun)
Jae Hyung Choi, Yong Beom Park and Hee Chul Woo: Department of Chemical Engineering, Pukyong National University, 365 Sinseon-ro, Namgu, Busan 608-737, Korea

Keywords: antimicrobial activity; Box-Behnken design; deoiled *Saccharina japonica*; green synthesis; response surface methodology; silver nanoparticles.

1 Introduction

In recent years there has been increasing attention on the preparation and study of silver nanoparticles (AgNPs), which has rapidly improved due to their electronic, photo electrochemical, chemical, magnetic, antibacterial, catalytic, and bioactive properties [1]. It has engrossed a demanding exploration because of their valuable applications in drug delivery, biomedical, agriculture, foodstuff industry, and fabric industries as an anti-microbial mediator [2]. In the modern era, green synthesis of nanoparticles (NPs) has got a lot of consideration over chemical and physical production, as it is a clean, eco-friendly, non-hazardous, non-toxic, renewable high-energy efficient material, their fate and transport as well as the development of real-time monitoring and process control to avoid or minimize accidents [3]. Consequently, the combination of green chemistry ideologies into nanotechnology is vital where the growth of nanotechnology might profit from a greener methodology that endorses both safety and performance [4]. The production of NPs was considered as a key factor in biologically orientated experiments which improve the nanotechnology field. The biological or green-based synthesized AgNPs were produced by using bacteria, fungi, algae, plants, and biomaterials [5].

Marine macroalgae are characterized into green (chlorophytes), brown (phaeophytes), and red (rhodophytes), which live either in marine or freshwater environment [6]. Seaweeds are commonly used as regular foods due to their nutritional value, including lipids, minerals, vitamins, and bio-functional materials such as proteins, polysaccharides, and polyphenols. It also has several medical benefits such as inflammation, cancer, allergy, thrombosis, diabetes, lipidemia, hypertension, obesity, and other

degenerative diseases [7]. Recently, many reports suggest that seaweeds can be used as a bio-factory for synthesis of silver and gold nanoparticles [8]. The brown seaweeds are rich in polysaccharides such as alginate and fucoidans and also have a complex cell wall which helps in the uptake of heavy metals [9]. The functional groups present in the brown seaweeds, particularly the carboxyl groups, help in the recovery of metals, and some reports say it may account for 60–80% of the dry weight of the biomass. Other functional groups that are in the seaweed cell walls are sulfhydryl, amino, and sulfonate [10].

Hydrogen peroxide (H_2O_2) is a strong oxidizing agent which is widely used in food, pharmaceutical, cosmetics, wood, and pulp industries. However, the exposure and presence of even a small of amount of H_2O_2 in a process stream results in various health and environmental hazards due to its toxicity [11]. Therefore, it is essential to develop accurate and fast methods to detect H_2O_2. Bera and Raj [12] used triangular silver nanoplates for the detection of H_2O_2. Wang and Yun [13] developed a non-enzymatic sensor for H_2O_2 based on the electrodeposition of AgNPs on poly(ionic liquid)-stabilized graphene sheets, and they demonstrated the detection of H_2O_2 in commercially available products such as honey and milk. Recently, Mohan et al. [14] exploited the AgNPs synthesized from dextrose for the optical sensing of H_2O_2.

Saccharina species are well known to be found in the deep sea of South Korea and Japan. It is one of the main kelps grown in large areas of marine water; additionally, it offers accommodation for sea organisms, soothes the nutritious salt content, increases marine water quality, and maintains the underground sediments. *Saccharina* are commonly utilized as a food material in Asian countries [15]. Specifically, *Saccharina japonica* (Areschoug) Lane, Mays, Druehl, and Saunders, kelp are grown near the sea shore of Gi-jang, Busan, South Korea; traditionally, it is an essential part of Korean foods and this species also has high industrial value. To date, there is no report on the synthesis of AgNPs using deoiled *S. japonica* aqueous extracts. In this study, we made an attempt to optimize the process variables, namely, reaction time, temperature, and concentration of $AgNO_3$ that affect the biosynthesis of AgNPs using Box-Behnken response surface design.

2 Materials and methods

2.1 Chemicals

Silver nitrate, chlorogenic acid, and rutin were procured from Sigma-Aldrich (St. Louis, MO, USA). Milli-Q water (Milli-Pore, Bedford, MA, USA) was used in this study. All other chemicals used in this experiment were analytical and HPLC (high-pressure liquid chromatography) grade.

2.2 Biosynthesis of silver nanoparticles

Sivagnanam et al. [16] have been working on the extraction of seaweed oil from *S. japonica*, which was obtained from Guemil-eup, Wando-gun, Jeollanam-do, Republic of Korea. The Sc-CO_2 process was used to extract oil from brown seaweed; the residue obtained after the process is called Deoiled *Saccharina japonica* powder (DSP). In this study, DSP was used to synthesis the AgNPs as shown in Figure 1. DSP (1 g) was mixed in 100 ml Milli-Q water, stirred for 200 rpm, and kept at 100°C for 20 min. Then it was filtered using 0.2 µm filter paper Merck (Darmstadt, Hesse, Germany) and kept in 4°C for further processing.

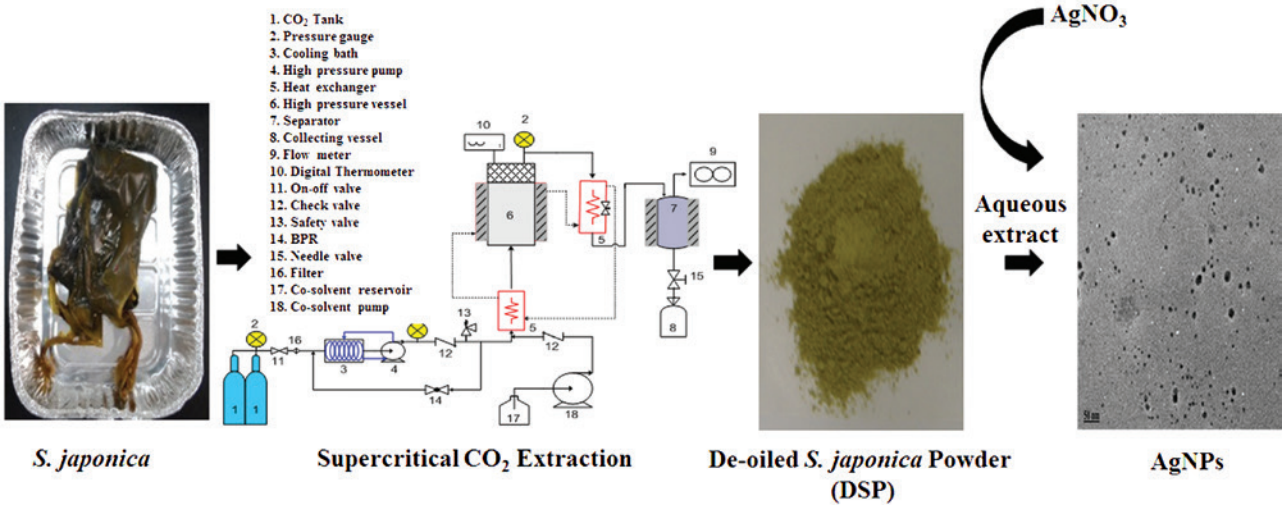

Figure 1: Schematic drawing of green synthesis diagram of AgNPs.

2.3 Biosynthesis and optimization of nanoparticles by response surface methodology (RSM)

The RSM was used to estimate the various effects of reaction conditions and to optimize those conditions. In this experiment a three-level box-behnken design (BBD) with three numeric factors was used. Fifteen runs with three replicates at a central point was used in this design. Independent variables used in trials were $AgNO_3$ concentration (A, 1–4 mmol l^{-1}), temperature (B, 40–60°C), and reaction time (C, 30–60 min). The biosynthesis was done by mixing 50 ml of various $AgNO_3$ concentrations, and 50 ml of aqueous DSP extract was added and the mixture kept at 200 rpm for all the conditions. The range of the coded variables was kept from –1 to 1 to normalize each reaction parameters, so that it will affect each response evenly [17]. The following equation for each variable was given [18]:

$$X = \frac{(x_i - x_o)}{\Delta x} \quad (1)$$

where X is the coded value, x_i is the actual value, x_o is the actual value in the center of the domain, and Δx is the increment of x_i corresponding to a variation of unit of X. The coded and natural values of independent variables used in BBD are presented in Table 1. The response variables were fitted to the second-order polynomial model [Eq. (2)] which is normally described as a relationship between the responses and the independent variables:

$$Y = \beta_0 + \sum_{i=1}^{3} \beta_i X_i + \sum_{i=1}^{3} \beta_{ii} X_i + \sum \sum_{i<j=1}^{3} \beta_{ii} X_i X_j \quad (2)$$

where Y represents the response variable, X_i and X_j are the independent variables affecting the response, and β_0, β_i, β_{ii}, and β_{ij} are the regression coefficients for intercept, linear, quadratic, and interaction terms. In this experiment the response was AgNPs size, and its optimized reaction conditions were determined. Desirability function was applied to select the best conditions and behavior of various responses [18]. Design-Expert v.7 (Stat-Ease, Minneapolis, Minnesota, USA) was used to obtain experimental design and multiple linear regression analysis.

2.4 Characterization of silver nanoparticles

The synthesized aqueous AgNPs were freeze dried, powdered, then mixed with potassium bromide and measured using the Spectrum GX FT-IR (Perkin Elmer Inc., Waltham, MA, USA) equipped with a DTGS detector. IR spectra were recorded within the range of 400–4000 cm^{-1}.

Table 1: Experimental domain with natural and coded values of independent variables used in Box-Behnken design.

Factor	Variable	Coded variable level		
		Low	Center	High
		–1	0	1
A	$AgNO_3$ (mmol l^{-1})	1.00	2.50	4.00
B	Temperature (°C)	40.00	50.00	60.00
C	Reaction time (min)	30.009	45.00	60.00

The synthesized aqueous AgNPs were observed by UV-vis spectroscopy using Shimadzu (Kyoto, Honshu, Japan) (Model No. UV-1800) double-beam UV-vis spectrophotometer. The AgNPs powder was used for X-ray diffraction (XRD) analysis (X'Pert-MPD, Philips, Eindhoven, Netherlands) at 40 kV/30 mA using constant scanning 2θ mode. AgNPs were fixed on case ends with double-sided sticky tape covered with platinum in a spit coater and viewed in a field emission scanning electron microscopy (FETEM) (JSM-6700, JEOL, Akishima, Tokyo, Japan). For high-resolution transmission electron microscopy (HRTEM) imaging, a droplet of aqueous AgNPs was kept on carbon-coated copper grids and dried under an infrared lamp (JEM 1010, JEOL, Akishima, Tokyo, Japan) (AC voltage 80.0 kV). In addition, the existence of silver ions in the synthesized AgNPs was investigated by energy dispersive X-ray (EDX) combined with FETEM.

2.5 Antimicrobial activity against food pathogens

2.5.1 Agar well diffusion: Antimicrobial activity of the synthesized AgNPs against six food borne-bacteria, three each from Gram-positive and Gram-negative bacteria (*Escherichia coli* ATCC 25922, *Pseudomonas aeruginosa* ATCC 9027, *Salmonella typhimurium* KCCM 11862, *Staphylococcus aureus* ATCC 6538p, *Listeria monocytogenes* ATCC 7644, and *Bacillus cereus* ATCC 13061), and two fungal strains (*Candida albicans* ATCC 10231 and *Aspergillus brasiliensis* ATCC 16404) were studied using well diffusion method [16]. Some 20–100 µl of AgNPs was added into the well [powder was mixed with 10% dimethyl sulphoxide (DMSO)] with 20 µl of 10% DMSO to serve as a negative control. Each plate was incubated at 37°C for 24–48 h, and the zone of inhibition was measured by observing the diameter of the clear zone. Each experiment was conducted in triplicate.

2.5.2 Minimal inhibitory concentration/minimum bactericidal concentrations: The synthesized AgNPs were examined for their minimal inhibitory concentration (MIC). Some 0.5 ml of different concentrations of AgNPs were prepared using DMSO. Then it was mixed with 50 µl of 24 h old bacterial culture and 48 h old fungus and then incubated at 37°C for 24–48 h. To analyze the MIC, turbidity of microbial growth was observed in each concentration. The MIC was determined by subculturing the MIC dilutions onto the sterile agar plates. The low concentration of the AgNPs which inhibits the growth of bacteria and fungus were spotted and measured. Minimum bactericidal concentration (MBC) is read as the lowest concentration of antimicrobial agent that kills all microorganisms, with complete absence of microbial growth. Each experiment was conducted in triplicate [19].

2.6 HPLC analysis of phenolic compounds

The HPLC analysis was conducted using a Waters 600 E HPLC system (Milford, MA, USA) equipped with a tunable absorbance detector (Waters 484). The amounts of phenolic acids in the samples were determined with a method previously reported by Kim et al. [20] with slight modification. The phenolic content in the aqueous AgNPs was determined by reversed-phase HPLC with mobile phase of distilled water with 0.1% glacial acetic acid (solvent A) and acetonitrile with 0.1% glacial acetic acid (solvent B) the detector was set at 280 nm. For sample preparation, briefly, an aliquot of aqueous AgNPs extracts was filtered with a 0.22 µm membrane filter.

2.7 Hydrogen peroxide-sensing capacity of silver nanoparticles

The sensing capacity of AgNPs to detect H_2O_2 was done according to Bera and Raj [12]. The initial spectrum of appropriately diluted aqueous AgNPs (3 ml) was noted using the spectrophotometer. About 1 ml of 20 mM H_2O_2 was added to the aqueous AgNPs solution and thoroughly mixed. The spectrum readings were taken at regular intervals, and the change in spectra was noted.

3 Results and discussion

3.1 Data analysis and evaluation of RSM model

The trials were done according to BBD for optimizing the conditions to produce AgNPs size using various conditions, and the obtained responses are listed in Table 2, in which randomly 15 trails were made using BBD. The trial arrangement was kept random to reduce the effects of the uncontrolled factors. The experimental error was estimated by having three trials. The sum of squares and polynomial was obtained from the BBD model. We can say that this is a kind of sequential use of highly fractionated factorial designs [18]. The responses of average size of AgNPs were considered in studying the effect of process variables. AgNPs size and the independent variables were used to develop one empirical model, which is presented by Eq. (3) as follows:

$$\begin{aligned}\text{AgNPs particle size} = {} & 33.53 - 40.16A + 1.24B + 2.84C \\ & + 1.23AB + 3.58AC + 0.51BC \\ & + 21.72A^2 - 1.26B^2 + 1.90C^2 \end{aligned} \quad (3)$$

The AgNPs size ranged from 14.77 to 105.00 nm (Table 2). A previous report in brown seaweed *Sargassum wightii* was used to produce AgNPs, and the obtained particle size was found to be around 5–22 nm [21]. Another report in *Sargassum muticum* showed that the obtained AgNPs size was measured to be 5–15 nm approximately; it was also found to be well dispersed with a spherical shape [22]. Shao et al. [23] reports that structure and size of obtained NPs was connected with interfaces between bio-materials such as proteins, polysaccharides, and phenolic acids with iron particles.

3.2 Model fitting

Experimental data for the response of AgNPs was fitted to a second-order polynomial model [Eq. (2)], and multiple regression coefficients were calculated for all reactions using the arithmetical method named as method of least squares which denotes a multiple regression technique creating the lowermost average size [7, 24]. In Table 3, the regression coefficient of each model with responses was shown and analysis of variance (ANOVA) is presented in Table 4. The (R^2) coefficients of multiple determinations for AgNPs size was 0.9991; it confirms that the equation model offers worthy illustration of experimental data. $R^2 \sim 1$ in a good statistical model [25] suggests that the model is 99.91% accurate. Moreover, the response for significant regression of the model was $p < 0.05$ (Table 4), which was obtained by mathematical models. Lack of fit testing confirmed adequacy of fitting experimental data to a second-order polynomial model in case of influence of independent variables on investigated responses, where

Table 2: Box-Behnken experimental design with natural and coded reaction conditions and experimentally obtained values of AgNPs size.

Run	A, $AgNO_3$ (mmol l^{-1})	B, Temperature (°C)	C, Reaction time (min)	AgNPs size (nm)	
				Experimental	Predicted
1	2.5 (0)	40 (−1)	30 (−1)	30.91	30.60
2	4 (1)	50 (0)	60 (1)	105.00	103.72
3	2.5 (0)	50 (0)	45 (0)	33.82	33.52
4	2.5 (0)	50 (0)	45 (0)	34.09	33.52
5	4 (1)	50 (0)	30 (−1)	92.04	90.88
6	1 (−1)	40 (−1)	45 (0)	14.77	13.80
7	1 (−1)	60 (1)	45 (0)	15.30	13.83
8	2.5 (0)	60 (1)	30 (−1)	31.86	32.05
9	2.5 (0)	40 (−1)	60 (1)	35.45	35.25
10	4 (1)	60 (1)	45 (0)	95.65	96.61
11	4 (1)	40 (−1)	45 (0)	90.22	91.68
12	2.5 (0)	50 (0)	45 (0)	32.67	33.52
13	1 (−1)	50 (0)	30 (−1)	16.45	17.72
14	2.5 (0)	60 (1)	60 (1)	38.45	38.76
15	1 (−1)	50 (0)	60 (1)	15.09	16.24

Table 3: Estimated coefficients of the fitted second-order polynomial model for AgNPs size.

Regression coefficient	Response
β_0	33.53[a]
Linear	
β_1	40.16[a]
β_2	1.24
β_3	2.84
Cross product	
β_{12}	1.23
β_{13}	3.58
β_{23}	0.51
Quadratic	
β_{11}	21.72[a]
β_{22}	−1.26
β_{33}	1.90

[a]p Value is <0.01 level.

p-value for lack of fit was insignificant ($p > 0.05$) (Table 4). The experimental data were used to create the response surface with three-dimensional (3D) plots and regression equations which can forecast response values from experimental data [Eq. (3)]. ANOVA confirms that equations can adequately describe the behavior of AgNPs size [26].

3.3 Response surface analysis

The predicted model versus experimental values for AgNPs size is shown in Table 2. Calculation of the linear correlation coefficient indicated a realistic arrangement between the model and experimental values. The predicted values were quite close to the experimental values. So it suggests that the designed model was realistic. Figure 2 shows the

Table 4: ANOVA of the fitted second-order polynomial model for AgNPs size.

Source	Sum of squares	Degree of freedom	Mean square	*F* value	p value Probability > *F*
Model	14813.54	9	1645.95	612.74	<0.0001
A-Silver nitrate	12904.21	1	12904.21	4803.84	<0.0001
B-Temperature	12.28	1	12.28	4.57	0.0856
C-Reaction time	64.58	1	64.58	24.04	0.0045
AB	6.00	1	6.00	2.23	0.1952
AC	51.27	1	51.27	19.08	0.0072
BC	1.05	1	1.05	0.39	0.5591
A^2	1741.54	1	1741.54	648.32	<0.0001
B^2	5.86	1	5.86	2.18	0.1998
C^2	13.34	1	13.34	4.96	0.0764
Residual	13.43	5	2.69		
Lack of fit	12.29	3	4.10	7.21	0.1243
Pure error	1.14	2	0.57		
Correlation total	14826.97	14			

The coefficient of determination (R^2) of the model was 0.9991.

3D surface plots for the experimental factors with response variables. The 3D images were useful to investigate the relationship between the response and effects of the factor. It also shows that the surface response was created to show how well the AgNPs size were varied with various factors using quadratic polynomial equations obtained from regression analysis. Figure 2A shows the effects of temperature and $AgNO_3$ concentration on the AgNPs size. The temperature does not have that much influence on the production of AgNPs size, while the $AgNO_3$ concentration has an effect. Figure 2B shows the effects of reaction time and $AgNO_3$ concentration on the AgNPs size. AgNPs ion concentration seldom exhibited an effect on the bulk density. Figure 2C represents the effects of temperature and reaction time on the AgNPs size. The effect of reaction time on the AgNPs size was not very significant, though the AgNPs size significantly diminished with increasing reaction temperature. So Figure 2 confirms that all the factors examined are interconnected. Validation of the model showed a similar deviation between the predicted vs. actual (Figure 2D), which is subject to trial conditions in which the experiments were run. Earlier, Muralidhar et al. [27] and Khajeh [28] have reported that an elliptical or saddle nature of 3D contour plots represents regression equation investigating interaction among variables which determine optimum parameters. In conclusion, reaction

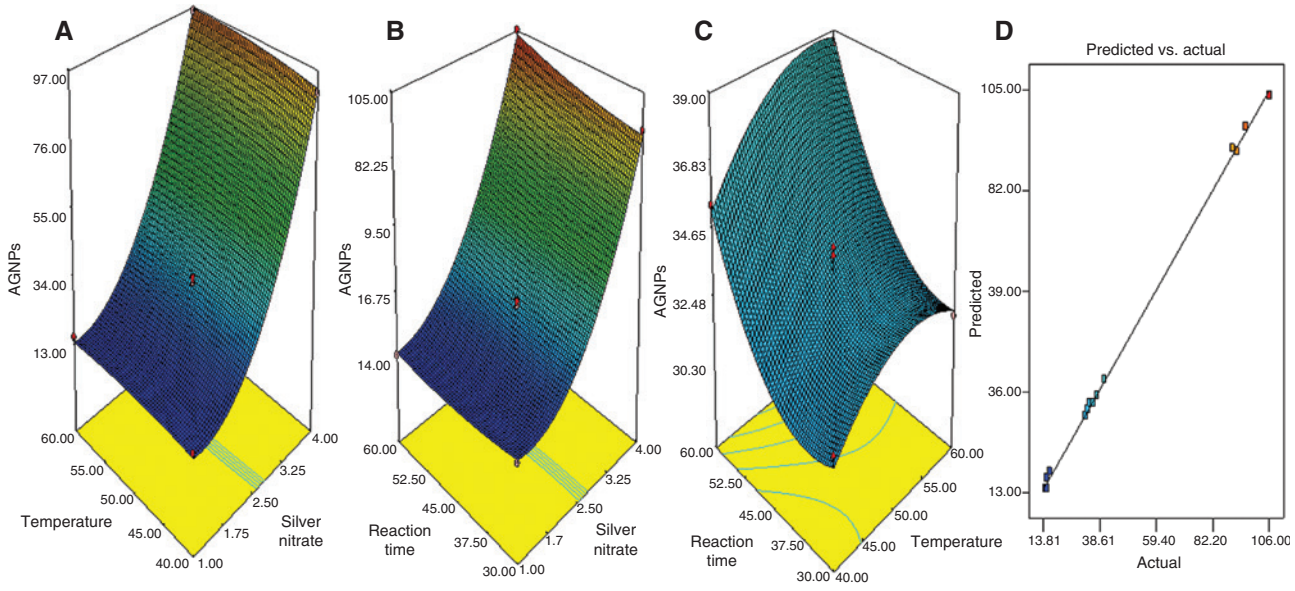

Figure 2: (A–C) Response surface plots showing combined effects of silver nitrate concentration, temperature, and reaction time on size of AgNPs and (D) predicted vs. actual plot graph.

time and $AgNO_3$ concentration had the main effect, while the temperature has not that much effect on the investigated response. The elliptic curve indicated that the two factors exhibited obvious interaction effects. Complex synergy effects occurred with the reaction time, temperature, and $AgNO_3$ concentration.

3.4 Optimization of AgNPs production

To produce AgNPs with a desired size in large-scale process, optimized conditions were necessary, and it also reduces the cost. So the production of AgNPs with several variables must be optimized. The production of AgNPs using green synthesis has definite benefits when compared with chemical synthesis; however, reaction time, temperature, and $AgNO_3$ concentration are the most significant variables in order to get sufficient product [29]. The $AgNO_3$ concentration has a significant impact to produce smaller or larger particle size, so to optimize $AgNO_3$ concentration, there should be a necessary step to produce desired size of AgNPs at the industrial scale. Optimized conditions for smaller size of AgNPs are presented in Table 2. To optimize the three factors at equal time desirability function was engaged, and elevated conditions were the $AgNO_3$ concentration of 1.51 mM, temperature of 40°C, and reaction time of 45 min. The achieved AgNPs size at this experimental point was 14.77 nm, and predicted size was 13.80 nm, while desirability was 0.9611. Since temperature and $AgNO_3$ concentration has significant effects, to produce the spherical-shaped AgNPs, it would be much easier to operate on low temperature and low $AgNO_3$ concentration which will not affect the size of AgNPs significantly.

3.5 Characterization of silver nanoparticles

The AgNPs were formed when aqueous DSP extract was added with aqueous silver nitrate. The synthesis of AgNPs was carried out with UV-vis spectroscopy using Shimadzu (Model No. UV-1800). The primary characterization of synthesized nanoparticles by UV–vis spectroscopy has proven to be a very valuable technique for the analysis of nanoparticles [30]. UV-vis absorption spectra displayed an extensive surface plasmon resonance at 420 nm (Figure 3A). Early reports showed that spherical AgNPs were observed in the area around 400–420 nm in the UV-vis spectra [31]. AgNPs showed yellowish brown color in aqueous solution due to excitation of surface plasmon vibrations [32]. After reaction the aqueous AgNPs extracts were kept in a dark room overnight, while the reaction mixture changed into a dark brown color solution which indicates the AgNPs synthesis (Figure 3B).

Further confirmation of Fourier transform infrared (FTIR) result suggests possible materials present in AgNPs that are liable for coating and lead to efficient stabilization of AgNPs. The FTIR spectral analysis (Figure 4A)

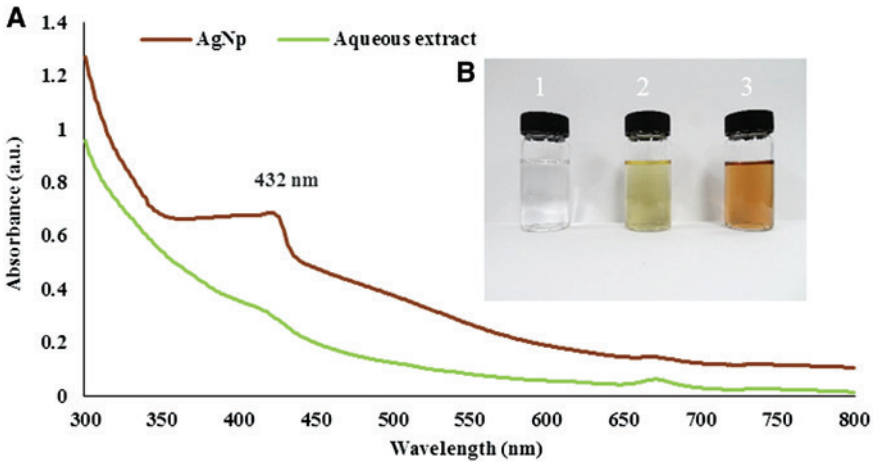

Figure 3: (A) UV-visible spectrum of optimized AgNPs (1 mM $AgNO_3$, 40°C, and 45 min) at the end of the reaction with the extract of deoiled *Saccharina japonica* (DSP) and aqueous solution of $AgNO_3$. (B) (1) $AgNO_3$ solution, (2) DSP aqueous extracts, and (3) after reaction.

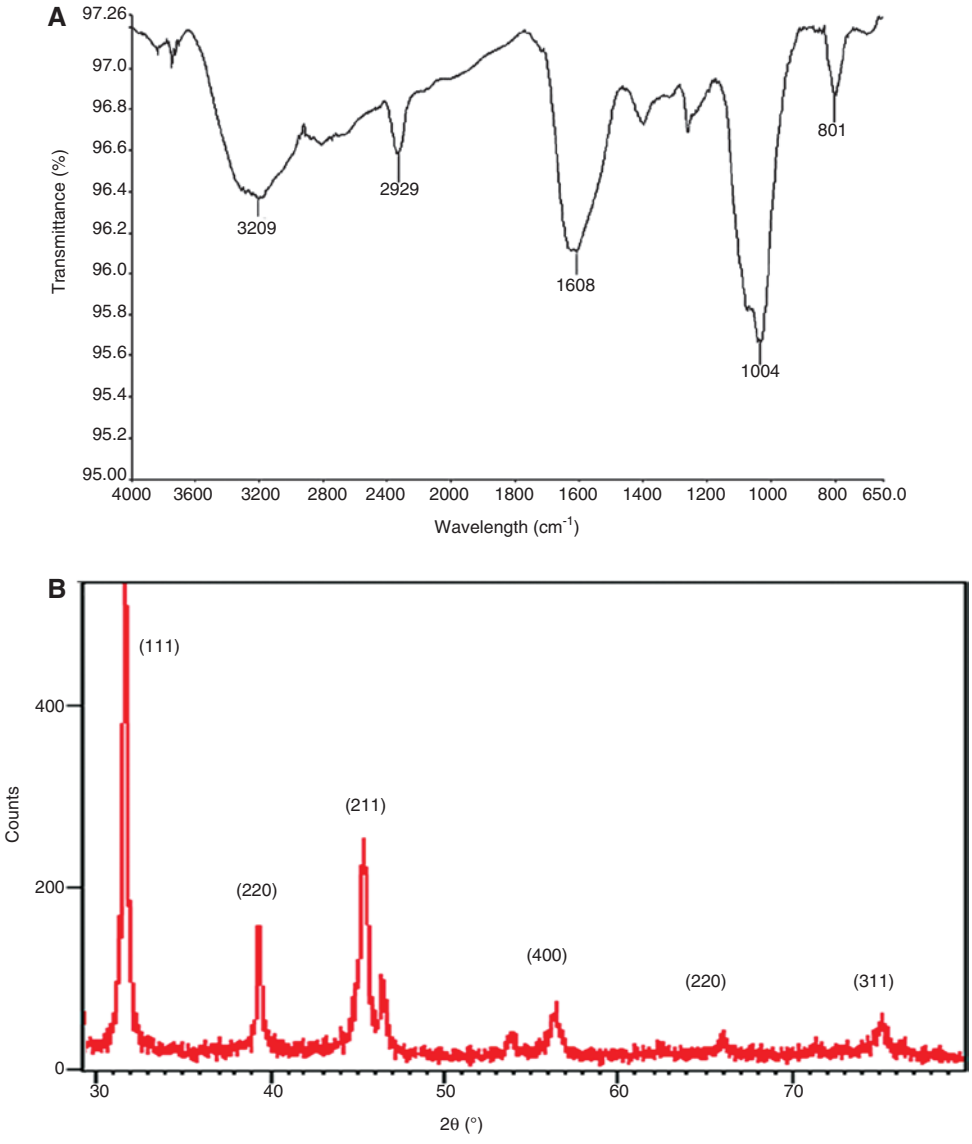

Figure 4: (A) FT-IR spectrum, (B) X-ray diffraction pattern of optimized AgNPs (1 mM $AgNO_3$, 40°C, and 45 min).

Table 5: Characteristic XRD parameters of bio-synthesized optimized AgNPs (1 mM $AgNO_3$, 40°C, and 45 min) from the DSP extract.

2θ (°)	Plane (*h*, *k*, *l*)	Interplanar spacing (nm)	Lattice parameter (nm)	FWHM (rad)	Crystallite size (nm)
31.69	(1, 1, 1)	0.282	4.040	0.0236	6.89
39.37	(2, 2, 0)	0.228	3.970	0.0118	15.18
45.37	(2, 1, 1)	0.199	4.071	0.0236	8.35
56.38	(4, 0, 0)	0.163	4.026	0.0472	5.30
66.07	(2, 2, 0)	0.141	4.017	0.0236	14.47
75.09	(3, 1, 1)	0.126	4.004	0.0576	9.35

reveals the presence of absorption peaks at 3209, 2329, 1608, 1034, and 801 cm^{-1}. The biosynthesized AgNPs were observed in the existence of bands due to O–H stretching (3209 cm^{-1}), C=O stretching (2329 cm^{-1}), N–H bend (1608 cm^{-1}), C–N stretching (1034 cm^{-1}) and C–Br stretching (801 cm^{-1}). When the metal nanoparticles formed in the solution, they must be stabilized against the Van der Waals forces of attraction which may otherwise cause coagulation. FTIR analysis data confirm the presence of O–H stretching (3209 cm^{-1}) which may be responsible for reducing metal ions into their respective Ag^+ to Ag^0. The results of XRD patterns showed various size and types resulting in different peak position, heights, and widths. Three strong peaks were identified in the complete spectrum of XRD pattern with 2θ values ranging from 30 to 80 (Figure 4B).

XRD spectrum of the synthesized AgNPs shows the exact nature of the silver particles formed. The obtained XRD spectrum was compared with the standard, and it confirms the presence of NPs in the arrangement of nanocrystals, as supported by the peaks at 2θ values of 31.69°, 39.37°, 45.37°, 56.38°, 66.07°, and 75.09° corresponding to (1, 1, 1), (2, 2, 0), (2, 1, 1), (4, 0, 0), (2, 2, 0), and (3, 1, 1) planes for silver, respectively. Similar results were previously reported by Sukirtha et al. [33]. The size of the AgNPs was calculated by Debye-Scherrer equation [34] as follows:

$$S = k\lambda / \beta_{0.5} \cos\theta \quad (4)$$

where S is the crystallite size of AgNPs, λ is the wavelength of the X-ray source (1.54056 Å) used in XRD, $\beta_{0.5}$ is the full width at half maximum (FWHM) of the diffraction peak in radian, k is the Scherrer constant that varies from 0.9 to 1, and θ is the Bragg angle in radian. The various calculation parameters including the lattice parameter and crystal sizes are shown in Table 5. In the present XRD pattern, the average size of nanoparticles was calculated as 9.92 nm. The lattice parameters were 4.040, 3.970, 4.071, 4.026, 4.017, and 4.004 nm for (1, 1, 1), (2, 2, 0), (2, 1, 1), (4, 0, 0), (2, 2, 0) and (3, 1, 1) planes, respectively. The calculated values are concordant with the standard lattice parameter of 4.0729 nm for metallic silver [35]. For instance, Sathyavathi et al. [36] reported diffraction peaks at 44.50°, 52.20°, and 76.7° 2θ, which correspond to the (111), (200), and (220) facets of the face-centered cubic crystal structure. Also, Dubey et al. [37] noted that the size of silver nanocrystals as estimated from the full width at half-maximum of (111) peak of silver using the Scherrer formula was 20–60 nm.

The characteristics and sizes of the NPs were determined by HRTEM. Figure 5A–D shows that NPs are spherical, with a particle size range from 10 to 40 nm with an average particle size of 14.77 ± 0.25 nm (Figure 6). In previous reports, HRTEM images showed the biosynthesized AgNPs with spherical shape, and the size varied from 10 to 100 nm [38]. The results of EDX analysis are shown in Figure 5E. It also supports the presence of Ag. EDX graph showed the presence of the elemental Ag in the sample, which indicated the reduction of silver ions to elemental silver.

3.6 Antimicrobial activity

AgNPs are well known for their antimicrobial activity. The antimicrobial activity of biosynthesized AgNPs was investigated against various pathogenic organisms such as *E. coli*, *P. aeruginosa*, *S. typhimurium*, *L. monocytogenes*, *B. cereus*, *S. aureus*, *C. albicans*, and *A. brasiliensis* using well-diffusion method. The diameter for the zone of inhibition of each pathogen was measured and tabulated (Table 6). The AgNPs displayed good antimicrobial activity against bacterial and fungal strains; the results showed visible and clear zones of inhibition (Figure 7). The mean zones of inhibition ranged from 8 to 22 mm. The highest antimicrobial activity was observed against *S. aureus* showing 22 ± 0.05 mm at 100 µl/well. The zone of inhibition for all bacteria was found to be high in 100 µl/well. AgNPs have no activity against *P. aeruginosa* and *A. brasiliensis*. Sarkar et al. [39] stated that for *E. coli* and *S. aureus*,

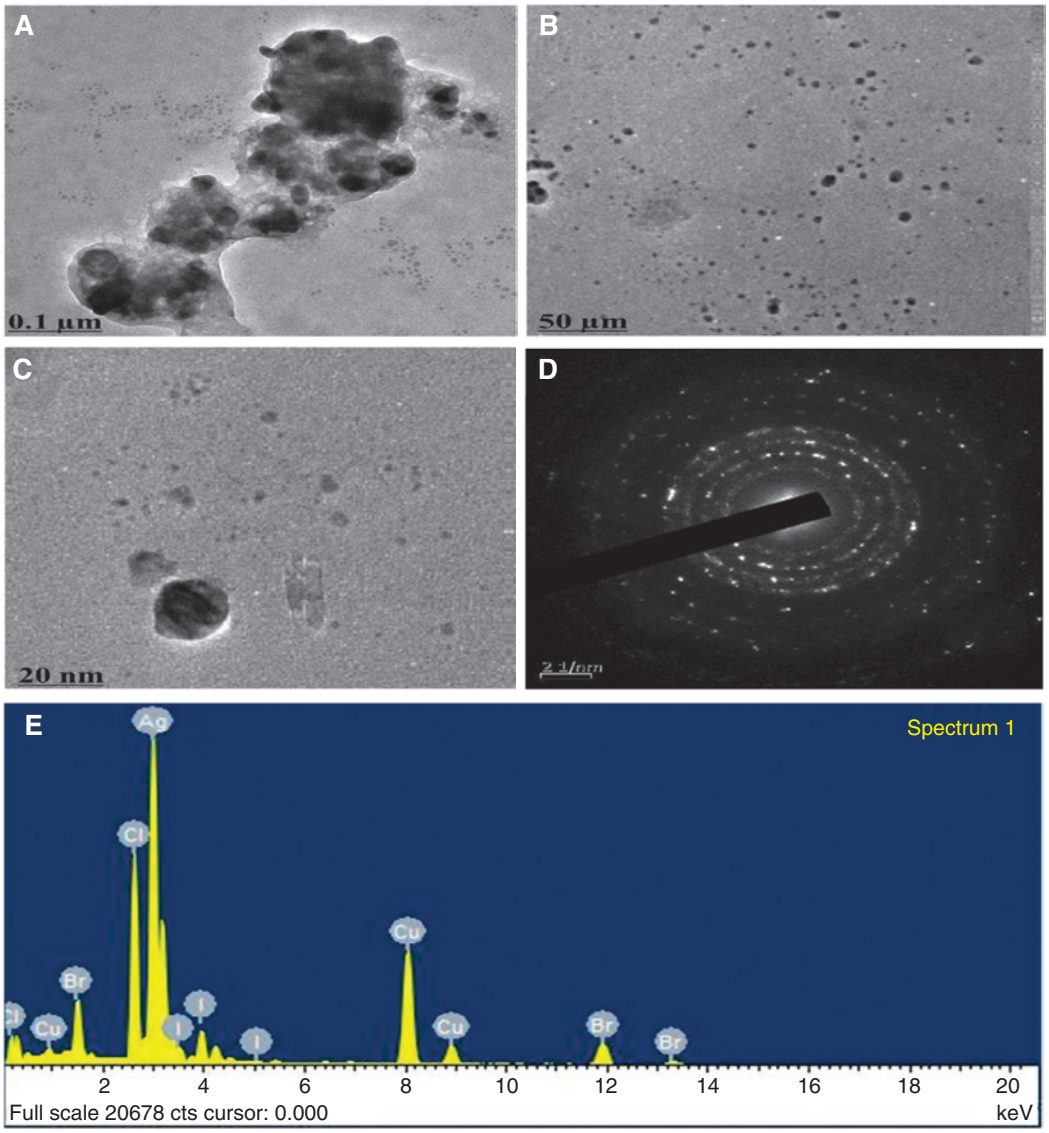

Figure 5: HR-TEM images: (A) 0.1 µm scale, (B) 50 nm scale, (C) 20 nm scale, (D) selected area diffraction pattern, and (E) EDX analysis of optimized (1 mM $AgNO_3$, 40°C, and 45 min) AgNPs synthesized by DSP extract.

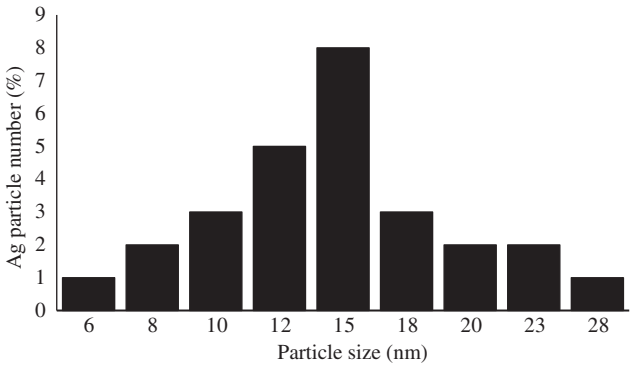

Figure 6: Particle size distribution under optimized conditions. The particle size distribution revealed that the particles ranged 15 nm had the maximum intensity, and thereafter the intensity was reduced. The average particle size was found to be 14.77 ± 0.25 nm.

AgNPs exhibit superior antimicrobial efficacy parallel to penicillin.

The MIC method was done by varying the concentrations of AgNPs. MIC was determined using various concentrations of AgNPs (5 µg/ml to 50 µg/ml). The results of MIC values for *E. coli* (6 ± 1.5 µl/ml), *S. typhimurium* (14 ± 4.2 µl/ml), *L. monocytogenes* (25 ± 4.6 µl/ml), *B. cereus* (25 ± 5.8 µl/ml), *S. aureus* (13 ±1.2 µl/ml), and *C. albicans* (16 ± 5.0 µl/ml) using AgNPs synthesized from DSP extracts are listed in Table 6. The MBC values for *E. coli* (11 ± 4.5 µl/ml), *S.typhimurium* (21 ± 3.4 µl/ml), *L. monocytogenes* (41 ± 2.9 µl/ml), *B. cereus* (45±8.7 µl/ml), *S. aureus* (21 ± 5.9 µl/ml), and *C. albicans* (28 ± 2.6 µl/ml) are shown in Table 6. Bankura et al. [40] reported that synthesized AgNPs (200 µg/ml) exhibit efficient antimicrobial

Table 6: Antimicrobial activity by well diffusion method, MIC and MBC of biosynthesized optimized silver nanoparticles (1 mM $AgNO_3$, 40°C, and 45 min) from optimized conditions.

Microorganisms	Well diffusion assay (mm diameter)					MIC (µl/ml)	MBC (µl/ml)
	20 (µl/well)	40 (µl/well)	60 (µl/well)	80 (µl/well)	100 (µl/well)		
E. coli	12±0.10	15±0.50	17±0.10	18±0.70	20±0.70	6±1.5	11±4.5
P. aeruginosa	ND	ND	ND	ND	ND	ND	ND
S. typhimurium	ND	ND	12±0.10	14±0.10	16±0.10	14±4.2	21±3.4
L. monocytogenes	ND	ND	8±0.25	10±0.08	16±0.25	25±4.6	41±2.9
B. cereus	ND	ND	ND	12±0.25	14±0.25	25±5.8	45±8.7
S. aureus	14±0.50	16±0.50	18±0.40	20±0.05	22±0.05	13±1.2	21±5.9
C. albicans	ND	ND	8±0.00	12±0.10	15±0.10	16±5.0	28±2.6
A. brasiliensis	ND	ND	ND	ND	ND	ND	ND

Values are expressed as mean ± SD. ND, not detected.

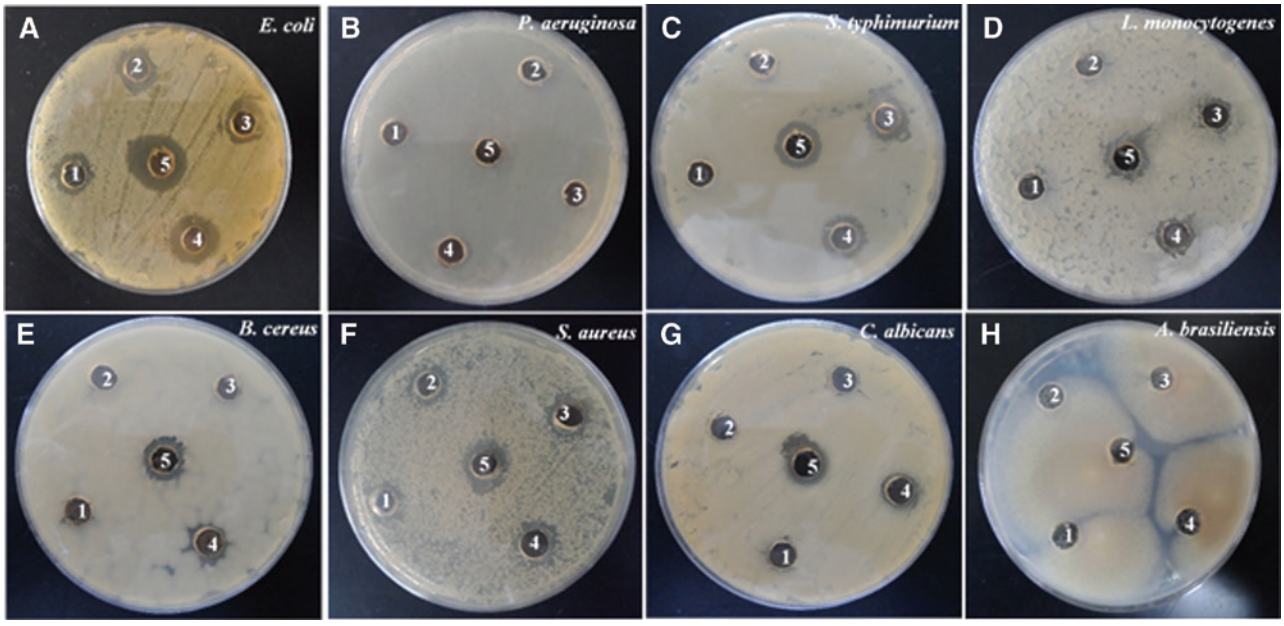

Figure 7: Antimicrobial activity of optimized AgNPs (1 mM $AgNO_3$, 40°C, and 45 min) synthesized by DSP on (A) *Escherichia coli*, (B) *Pseudomonas aeruginosa*, (C) *Salmonella typhimurium*, (D) *Listeria monocytogenes*, (E) *Bacillus cereus*, (F) *Staphylococcus aureus*, (G) *Candida albicans*, and (H) *Aspergillus brasiliensis*. Each plate shows (1) 20 µl of AgNPs, (2) 40 µl AgNPs, (3) 60 µl AgNPs, (4) 80 µl AgNPs, and (5) 100 µl AgNPs.

activity against *Bacillus subtilis*, *B. cereus*, *E. coli*, and *C. albicans* with inhibition zone diameters of 32, 28, 21, and 24 mm, respectively.

There are various mechanisms proposed in the literature for the antimicrobial effect of AgNPs. Patil et al. [41] claimed that the cell death arising out of exposure to AgNPs might be due to the cytoplasmic membrane disorganization and the consequent leakage of various biomolecules such as amino acids, protein, and carbohydrates. The change in membrane permeability caused by the action of AgNPs as a function of conductivity was studied by Krishnaraj et al. [42]. Their study concluded that the high conductivity of cells treated with SNPs was due to the release of cellular components present inside the cells. Tamboli Tamboli et al. demonstrated [43] demonstrated that the antimicrobial effect of AgNPs was due to the breakage of double-stranded DNA molecules present in the bacteria. The pronounced antibacterial effect in the present study may provide a new platform in the field of development of new antibacterial drugs.

3.7 HPLC analysis of phenolic compounds

Seaweeds are well known for their biological activities; these activities are obtained from their secondary

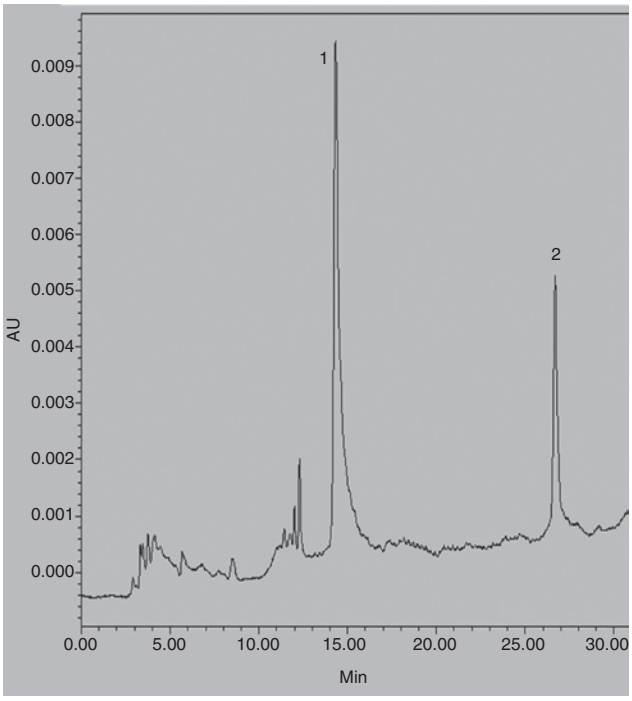

Figure 8: HPLC-UV-vis chromatogram of DSP extracts at 280 nm. Peaks: (1) chlorogenic acid and (2) rutin.

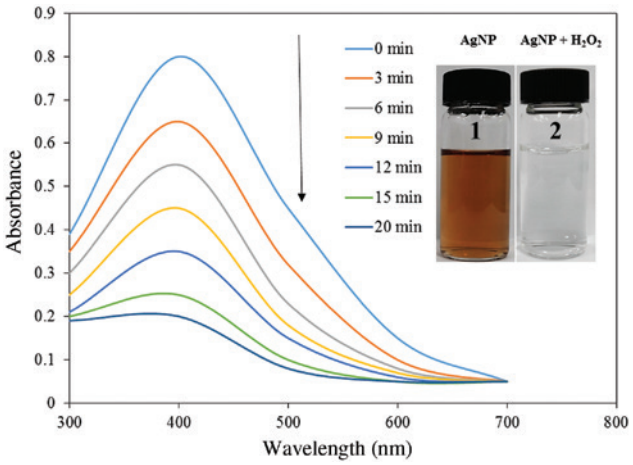

Figure 9: Effect of AgNPs (1 mM $AgNO_3$, 40°C, and 45 min) synthesized using DSP extracts on 20 mM H_2O_2 solution as a function of time.

metabolites. In that polyphenol is a major compound, which also has the properties of reducing agents. To detect phenolic acids in synthesized aqueous AgNPs extracts, HPLC analysis was carried out. The chromatogram of AgNPs extracts shows two different peaks with retention times of 15.0 and 26.0 min, which correspond to chlorogenic acid and rutin; the obtained chromatogram is shown in Figure 8. Among the known compounds, chlorogenic acid concentrations were found to be higher than the other phenolic acids. Therefore, it is clear that chlorogenic acid and rutin are the main components involved in the biosynthesis of AgNPs. Onofrejová et al. [44] stated that lower quantity of protocatechuic, *p*-coumaric, vanillic, caffeic, and chlorogenic acids were found in marine macroalgae. Another report identified polyphenolic compounds such as catechins (gallocatechin, epicatechin, and catehin gallate) and flavonol that are present in various brown, green, and red seaweeds [45].

The HPLC result confirmed the active participation of polyphenols in formation and stabilization of AgNPs. A previous report [46] showed that some polyphenols which contain hydroxyl groups support the formation of silver ions by reduction method; at the same time those polyphenols are oxidized to form its own quinine structure. Conversely, another report showed [47] that the interaction among polyphenols and metal ion was not studied properly. However, according to the principle, when hard ligands (hydroxyl groups present in polyphenols/–OH) come in contact with soft metal complexation is not favored instead, soft metal ion undergoes reduction. The soft ligands (carbonyl groups with polyphenols/–C=O) are formed when the hard ligands (–OH) undergo oxidation during the reaction synchronization that occurred with AgNPs due to the electrostatic interaction and stabilize the particles by controlling the growth of the particles [48].

3.8 Hydrogen peroxide-sensing capacity of AgNPs

The ability of AgNPs to detect the presence of H_2O_2 in a sample was affirmed by adding 1 ml of 20 mM H_2O_2 to 3 ml of appropriately diluted AgNPs. The spectrum was recorded as a function of time at regular intervals. As shown in Figure 9, a decreasing trend in absorbance was observed as the time increased and eventually the characteristic silver peak at 415 nm disappeared. It was apparent from the inset in Figure 9 that the color intensity of the AgNPs (vial 1) faded and finally became colorless (vial 2) after 20 min. This confirmed the ability of AgNPs to decompose H_2O_2 thus providing a means of sensing its composition. The results obtained in this study are in accordance with the previous study [11]. The connection between the concentration of H_2O_2 and decrease in absorbance of AgNPs as a function of time could be used as a measure to rapidly detect the H_2O_2 in the unknown samples. According to Mohan et al. [14], the addition of AgNPs to H_2O_2 resulted in the formation of free radicals which commenced the degradation of the AgNPs. Subsequently, Ag^0 was oxidized to Ag^+, and a decrease in absorbance was observed. These findings suggest that the

AgNPs can be successfully used to detect the concentration of H_2O_2 present in various samples.

4 Conclusions

To conclude, AgNPs were prepared through an innovative green synthesis. The current process holds benefits over other methods as follows: foremost, DSP is a vastly cost-effective reducing agent for the transformation of $AgNO_3$ to AgNPs. Secondly, RSM has potential applications in optimizing the different parameters facilitating synthesis of AgNPs possessing desired characteristic features. The optimized conditions were 1 mM $AgNO_3$, 40°C, and 45 min reaction time. These conditions produced spherical-shaped nanoparticle with a particle size of 14.77 nm. The obtained AgNPs also exhibited strong antimicrobial activity. The identification of phenolic acids in the aqueous AgNPs extract was confirmed by the HPLC analysis. The sensing capacity of the AgNPs toward H_2O_2 was also demonstrated. Hence, the AgNPs formed by this green method can be used as a probe to detect the presence of H_2O_2 in various samples. Besides, the proposed method is facile, rapid, and cost effective, and it has wide applications in commercial sectors. Due to the above-mentioned properties, the optimized condition is best fit for industrial scaling of AgNPs. To end with, this work delivers possible way of production in the area of green chemistry, nanotechnology, and materials science.

Acknowledgments: This work was supported by the Ministry of Oceans and Fisheries, Republic of Korea (20140559).

References

[1] Sharma VK, Yngard RA, Lin Y. *Adv. Colloid Interface* 2009, 145, 83–96.
[2] Jagtap UB, Bapat VA. *Ind. Crop. Prod.* 2013, 46, 132–137.
[3] Virkutyte J, Varma RS. *Chem. Sci.* 2011, 2, 837–846.
[4] Mulvihill MJ, Beach ES, Zimmerman JB, Anastas, PT. *Annu. Rev. Env. Resour.* 2011, 36, 271–293.
[5] Mandal D, Bolander ME, Mukhopadhyay D, Sarkar G, Mukherjee P. *Appl. Microbiol. Biot.* 2006, 69, 485–492.
[6] Azizi S, Ahmad MB, Namvar F, Mohamad R. *Mater. Lett.* 2014, 116, 275–277.
[7] Namvar F, Azizi S, Ahmad MB, Shameli K, Mohamad R, Mahdavi M, Tahir PM. *Res. Chem. Intermed.* 2015, 41, 5723–5730.
[8] Rajathi FAA, Parthiban C, Kumar VG, Anantharaman P. *Spectrochim. Acta A* 2012, 99, 166–173.
[9] Mata Y, Torres E, Blazquez M, Ballester A, González F, Munoz J. *J. Hazard. Mater.* 2009, 166, 612–618.
[10] Venkatesan J, Manivasagan P, Kim S-K, Kirthi AV, Marimuthu S, Rahuman AA. *Bioproc. Biosyst. Eng.* 2014, 37, 1591–1597.
[11] Tagad CK, Kim HU, Aiyer R, More P, Kim T, Moh SH, Kulkarni A, Sabharwal SG. *RSC Adv.* 2013, 3, 22940–22943.
[12] Bera RK, Raj CR. *J. Photoch. Photobio. A* 2013, 270, 1–6.
[13] Wang Q, Yun Y. *Microchim. Acta* 2013, 180, 261–268.
[14] Mohan S, Oluwafemi OS, George SC, Jayachandran V, Lewu FB, Songca SP, Kalarikkal N, Thomas S. *Carbohyd. Polym.* 2014, 106, 469–474.
[15] Yotsukura N, Nagai K, Kimura H, Morimoto K. *J. Appl. Phycol.* 2010, 22, 443–451.
[16] Sivagnanam SP, Yin S, Choi JH, Park YB, Woo HC, Chun BS. *Mar. Drugs* 2015, 13, 3422–3442.
[17] Baş D, Boyacı İH. *J. Food Eng.* 2007, 78, 836–845.
[18] Mourabet M, El Rhilassi A, El Boujaady H, Bennani-Ziatni M, El Hamri R, Taitai A. *Appl. Surf. Sci.* 2012, 258, 4402–4410.
[19] Gnanadesigan M, Anand M, Ravikumar S, Maruthupandy M, Ali MS, Vijayakumar V, Kumaraguru A. *Appl. Nanosci.* 2012, 2, 143–147.
[20] Kim MJ, Hyun J-N, Kim JA, Park J-C, Kim M-Y, Kim J-G, Chung IM. *J. Agr. Food Chem.* 2007, 55, 4802–4809.
[21] Shanmugam N, Rajkamal P, Cholan S, Kannadasan N, Sathishkumar K, Viruthagiri G, Sundaramanickam A. *Appl. Nanosci.* 2014, 4, 881–888.
[22] Azizi S, Namvar F, Mahdavi M, Ahmad MB, Mohamad R. *Materials* 2013, 6, 5942–5950.
[23] Shao Y, Jin Y, Dong S. *Chem. Commun.* 2004, 9, 1104–1105.
[24] Khajeh M, Sanchooli E. *Food Anal. Method.* 2010, 3, 75–79.
[25] Nyakundi EO, Padmanabhan MN. *Spectrochim. Acta A* 2015, 149, 978–984.
[26] Gunst RF. *Technometrics* 1996, 38, 284–286.
[27] Muralidhar R, Chirumamila R, Marchant R, Nigam P. *Biochem. Eng. J.* 2001, 9, 17–23.
[28] Khajeh M. *Food Chem.* 2011, 129, 1832–1838.
[29] Khajeh M, Kaykhaii M, Sharafi A. *J. Ind. Eng. Chem.* 2013, 19, 1624–1630.
[30] Rai M, Gade A. In *Industrial Exploitation of Microorganisms*, Saravanamuthu, R, Dubey, RC, Maheshwari, DK, Eds., I.K. International Publishing House Pvt. Ltd: New Delhi, 2010, p. 322.
[31] Shameli K, Ahmad MB, Al-Mulla EAJ, Shabanzadeh P, Bagheri S. *Res. Chem. Intermed.* 2015, 41, 251–263.
[32] Shankar SS, Sastry M. *J. Colloid Interf. Sci.* 2004, 275, 496–502.
[33] Sukirtha R, Thangam R, Gunasekaran P, Krishnan M, Achiraman S. *Process Biochem.* 2012, 47, 273–279.
[34] Culity, BD, Eds., In *Elements of X-ray Diffraction*, 2nd ed., Addison-Wesley Publishing Company, Inc.: London, 1978.
[35] Theivasanthi T, Alagar M. *Nano Biomed. Eng.* 2011, 4, 58–65.
[36] Sathyavathi R, Balamurali Krishna M, Venugopal Rao S, Saritha R, Narayana Rao D. *Adv. Sci. Lett.* 2010, 3, 1–6.
[37] Dubey M, Bhadauria S, Kushwah BS. *Dig. J. Nanomater. Bios.* 2009, 4, 537–543.
[38] Otari S, Patil R, Nadaf N, Ghosh S, Pawar S. *Mater. Lett.* 2012, 72, 92–94.
[39] Sarkar S, Jana AD, Samanta SK, Mostafa G. *Polyhedron* 2007, 26, 4419–4426.
[40] Bankura KP, Maity D, Mollick MMR, Mondal D, Bhowmick B, Bain MK. *Carbohyd. Polym.* 2012, 89, 1159–1165.

[41] Patil SV, Borase HP, Patil CD, Salunke BK. *Appl. Biochem. Biotech.* 2012, 167, 776–790.
[42] Krishnaraj C, Jagan E, Rajasekar S, Selvakumar P, Kalaichelvan P, Mohan N. *Colloid Surface B* 2010, 76, 50–56.
[43] Tamboli DP, Lee DS. *J. Hazard. Mater.* 2013, 260, 878–884.
[44] Onofrejová L, Vašíčková J, Klejdus B, Stratil P, Mišurcová L, Kráčmar S, Kopecký J, Vacek J. *J. Pharmaceut. Biomed.* 2010, 51, 464–470.
[45] Farvin KS, Jacobsen C. *Food Chem* 2013, 138, 1670–1681.
[46] Kumar KM, Mandal BK, Tammina SK. *RSC Adv* 2013, 3, 4033–4039.
[47] Kumar HAK, Mandal BK, Kumar TS, Madhiyazhagan P, Ghosh AR. *Spectrochim Acta A* 2014, 130, 13–18.
[48] Yoosaf K, Ipe BI, Suresh CH, Thomas KG. *J Phys Chem C* 2007, 111, 12839–12847.

Bionotes

Saravana Periaswamy Sivagnanam

Saravana Periaswamy Sivagnanam is currently pursuing his PhD degree at the Department of Food Science and Technology, Pukyong National University, Busan, Korea. His research interests include supercritical fluids, green biosynthesis of nanoparticles, and extraction of biomaterials from seaweeds.

Adane Tilahun Getachew

Adane Tilahun Getachew is a PhD candidate in Food Science and Technology, Pukyong National University, Korea. He has been working on extraction and characterization of bioactive compounds from coffee and coffee waste products using subcritical and supercritical fluids. He also has been working on encapsulation of bioactive compounds and flavors using encapsulation techniques that involve supercritical fluids. He has worked as a lecturer in the School of Chemical and Bioengineering, Addis Ababa University.

Jae Hyung Choi

Jae Hyung Choi is currently a postdoctoral fellow of the Institute of Cleaner Production Technology, Pukyong National University, where he is focused on integrated energy processes of macroalgal biomass. He obtained his BS (2008), MS (2010), and PhD (2015) degrees in the Department of Chemical Engineering, Pukyong National University, where he studied to develop pyrolysis and catalytic upgrading of macroalgae for liquid biofuel production under the guidance of Prof. Hee Chul Woo.

Yong Beom Park

Yong Beom Park is currently a PhD student in Pukyong National University, where he is focused on catalytic conversion of algal biomass into fuels and chemicals. He earned his Bachelor's degree in Chemical Engineering (2010) from Pukyong National University. He obtained his MS in Chemical Engineering from Pukyong National University in 2012.

Hee Chul Woo

Hee-Chul Woo is a Professor in the Department of Chemical Engineering, Pukyong National University, Korea, where he has taught since 1992. He received his BS degree (Inha University, Korea), MS degree (KAIST, Korea), and PhD degree (POSTECH, Korea) in Chemical Engineering and was a postdoctoral fellow at the University of California at Berkeley (1995–1996). In 2003 he was a visiting professor at Virginia Tech. His research interests cover heterogeneous catalysis, adsorptive desulfurization from gases and liquid fuels, and bioenergy production and integrated utilization of marine biomass. Woo is a general director of Aquatic Biomass Research Center.

Byung Soo Chun

Byung-Soo Chun received a doctor's degree in engineering from the University of South Australia, Australia. Now he is working as a Professor in the Department of Food Science and Technology, Pukyong National University, South Korea. His study fields are food engineering, chemical engineering, environmental engineering, separation engineering and reaction process engineering. His recent research topics are extraction and development of a process using supercritical fluid extraction using various natural resources.